

Reply to Referee #3

Thank you very much for your reviewing our manuscript and providing us valuable comments and suggestions.

This paper describes the new balloonborne instrument of cloud particles whose signal data is transmitted with a radiosonde to a ground station. The new sensor, CPS has capabilities to count particles larger than about 2 microns and to distinguish between cloud water droplets and ice crystals. The authors also mention some limitations using the test flight data in several launch sites.

However, it is not clear what levels of accuracy and range of uncertainties the new sensor has during the ascent flight. Although it might be the first light-weight costeffective balloonborne sensor over the cloud particle size range with a polarization function, the more quantitative evaluations are required for detecting/measuring variety of atmospheric particles.

I am ready to recommend the publication after the authors revise the manuscript taking into account the following comments, especially in terms of more supporting facts and figures which clearly indicate the measurement uncertainties and limitations. In my opinion, the manuscript will require a major revision for publication.

Please see below for our answers to your questions and concerns.

General comments:

Even if the main purpose of the paper is the demonstration of the new sensor, not quantitative discussions in detail, the basic performance of the sensor under the various atmospheric conditions is necessary since the CPS is a balloonborne sensor, rather than a ground-based instrument.

We have shown the basic performance of the CPS under various atmospheric conditions, i.e., midlatitude stratus (and cirrus) clouds, midlatitude precipitating clouds including mixed phase clouds, tropical thick cloud layers, and tropical upper tropospheric thin cirrus layers. We have also shown the results from laboratory experiments using various standard spherical particles. In the revised manuscript, we will also show the DOP distributions from the laboratory experiments (please see below for more details).

The manuscript is well written, however, I did not fully understand the strong points of this paper,

compared to the current airborne instruments of cloud particles. There are many other airborne instruments for cloud and aerosol particle measurements with the polarization function: for instance, CASPOL (Baumgardner et al., 2001, 2011; Glen and Brooks, 2013; Nichman et al., 2016), SID (Hirst et al., 2001; Cotton et al., 2010), and CPSPD (Baumgardner et al., 2014). These instruments have a higher sensitivity with more detectors, and those should be referred in the paper at least. Also, a polarization optical particle counter has developed and demonstrated (Kobayashi et al., 2014), although it covers the different measurement size range (0.5 – 10 microns) and is the ground-based instrument. Therefore the comparison in laboratory experiments with other sensor or instrument is strongly recommended to exhibit the basic performance of polarization measurements.

As discussed in the Reply to Referee #1, the weather balloon with a radiosonde is one of the major platforms for upper air sounding, measuring vertical profiles continuously from the surface up to the middle stratosphere in ~100 minutes. The radiosonde temperature and humidity measurements, including those from balloon-borne special hygrometers, have been well characterized by regular and special intercomparison campaigns (e.g. Nash et al., 2011; Vömel et al., 2016). The typical balloon ascent rate is ~5 m s⁻¹, which is much smaller than the speed of aircrafts, easing some of the technical challenges that aircraft instruments may face (e.g. shattering of ice crystals; Baumgardner et al., 2012). On the other hand, balloon instruments need to be disposable, operable with small batteries, and of small mass. These factors may result in technical challenges when developing balloon-borne cloud particle instruments. As described in Introduction, the masses of existing balloon-borne cloud particle instruments range from 1 to 6 kg except for COBALD whose mass is ~500 g. The CPS is a balloon-borne instrument with a small mass (~200 g) which is comparable to that of modern radiosondes, and thus is much more easily combined with a radiosonde to detect the “existence” of cloud particles. This may provide advances in understanding of cloud and water vapour processes because this gives us more opportunities to obtain a set of vertical profiles of temperature, humidity, and (existence of) cloud particles compared to the existing much heavier balloon-borne instruments. A combination of radiosonde temperature and humidity measurements with a ground-based or satellite particle remote-sensing measurements (as discussed in Section 3.4, for example) may be another way to obtain such a data set, but the measurement collocation is always an issue (e.g. Shibata et al., 2007). As a disposable instrument, there is limitation in number concentration measurements, though we propose a simple, partial correction algorithm and a simple algorithm to convert the number of count to number concentration. Furthermore, utilizing the polarization information, the CPS can distinguish between water, ice, and mixed phase cloud layers (i.e. for a group of particles; even for a single particle for particular conditions); more detailed explanation on this is given below.

In the revised manuscript, we will cite the aircraft instruments, the Cloud Aerosol Spectrometer with

Polarization (CASPOL; e.g. Nichman et al., 2016), the Small Ice Detector mark 2 (SID-2; e.g. Cotton et al., 2010), and the Cloud Particle Spectrometer with Polarization Detection (CPSPD; Baumgardner et al., 2014). We also cite the article by Baumgardner et al. (2012) and the textbook by Wendisch and Brenguier (2013) for recent developments on the aircraft instruments. Please note, however, that our focus is on developing a balloon-borne instrument flown with a radiosonde, and thus, as discussed above, there are several, very different technological issues and emphases. We will also point out that in the lidar community, the polarization information has been used for cloud measurements since the 1970s (Schotland et al., 1971; see also Sassen, 1991).

We are reluctant to extend our discussion to aerosol instruments. We would like to limit our discussion to balloon-borne cloud particle instruments, though we will add discussion on some aircraft cloud particle instruments as described above.

We have shown the results of our extensive laboratory experiments using standard spherical particles in Appendix A (and will add the DOP information from these experiments at the end of this appendix; please see below for more details). We are happy to participate in future laboratory and field intercomparison projects. Also, because the CPS is a commercial instrument, anyone who is interested can make independent evaluation by themselves.

References:

- Baumgardner, D., Avallone, L., Bansemer, A., Borrmann, S., Brown, P., Bundke, U., Chuang, P. Y., Cziczo, D., Field, P., Gallagher, M., Gayet, J.-F., Heymsfield, A., Korolev, A., Krämer, M., McFarquhar, G., Mertes, S., Möhler, O., Lance, S., Lawson, P., Petters, M. D., Pratt, K., Roberts, G., Rogers, D., Stetzer, O., Stith, J., Strapp, W., Twohy, C., Wendisch, M.: In situ, airborne instrumentation: Addressing and solving measurement problems in ice clouds, *Bull. Amer. Meteorol. Soc.*, 93 (2), ES29–ES34, doi:10.1175/BAMS-D-11-00123.1, 2012.
- Baumgardner, D., Newton, R., Krämer, M., Meyer, J., Beyer, A., Wendisch, M., Vochezer, P.: The Cloud Particle Spectrometer with Polarization Detection (CPSPD): A next generation open-path cloud probe for distinguishing liquid cloud droplets from ice crystals, *Atmos. Res.*, 142, 2-14, doi:10.1016/j.atmosres.2013.12.010, 2014.
- Cotton, R., Osborne, S., Ulanowski, Z., Hirst, E., Kaye, P. H., and Greenaway, R. S.: The ability of the Small Ice Detector (SID-2) to characterize cloud particle and aerosol morphologies obtained during flights of the FAAM BAe-146 research aircraft, *J. Atmos. Oceanic Technol.*, 27 (2), 290–303, doi: 10.1175/2009JTECHA1282.1, 2010.
- Nash, J., Oakley, T., Vömel, H., and Li, W.: WMO Intercomparison of high quality radiosonde observing systems, Yangjiang, China, 12 July - 3 August 2010, World Meteorological Organization

Instruments and Observing Methods, Report IOM-107, WMO/TD-No. 1580, available at <https://www.wmo.int/pages/prog/www/IMOP/publications-IOM-series.html>, 2011. [Last access: 19 August 2016.]

- Nichman, L., Fuchs, C., Järvinen, E., Ignatius, K., Höppel, N. F., Dias, A., Heinritzi, M., Simon, M., Tröstl, J., Wagner, A. C., Wagner, R., Williamson, C., Yan, C., Connolly, P. J., Dorsey, J. R., Duplissy, J., Ehrhart, S., Frege, C., Gordon, H., Hoyle, C. R., Kristensen, T. B., Steiner, G., McPherson Donahue, N., Flagan, R., Gallagher, M. W., Kirkby, J., Möhler, O., Saathoff, H., Schnaiter, M., Stratmann, F., and Tomé, A.: Phase transition observations and discrimination of small cloud particles by light polarization in expansion chamber experiments, *Atmos. Chem. Phys.*, 16, 3651-3664, doi:10.5194/acp-16-3651-2016, 2016.
- Sassen, K.: The polarization lidar technique for cloud research: A review and current assessment, *B. Amer. Meteorol. Soc.*, 72 (12), 1848-1866, doi:10.1175/1520-0477(1991)072<1848:TPLTFC>2.0.CO;2, 1991.
- Schotland, R. M., Sassen, K., and Stone, R.: Observations by lidar of linear depolarization ratios for hydrometeors, *J. Appl. Meteorol.*, 10 (5), 1011-1017, doi:10.1175/1520-0450(1971)010<1011:OBLOLD>2.0.CO;2, 1971.
- Shibata, T., Vömel, H., Hamdi, S., Kaloka, S., Hasebe, F., Fujiwara, M., and Shiotani, M.: Tropical cirrus clouds near cold point tropopause under ice supersaturated conditions observed by lidar and balloon-borne cryogenic frost point hygrometer, *J. Geophys. Res.*, 112, D03210, doi:10.1029/2006JD007361, 2007.
- Vömel, H., Naebert, T., Dirksen, R., and Sommer, M.: An update on the uncertainties of water vapor measurements using cryogenic frost point hygrometers, *Atmos. Meas. Tech.*, 9, 3755-3768, doi:10.5194/amt-9-3755-2016, 2016.
- Wendisch, M. and Brenguier, J.-L. (eds): *Airborne Measurements for Environmental Research: Methods and Instruments*, Wiley-VCH Verlag GmbH & Co. KGaA, Weinheim, Germany, 655 pp., doi:10.1002/97835276532182013, 2013.

If the CPS has an advantage of cloud phase determination in natural clouds, it remains ambiguous only from the frequency distribution of the degree of polarization (DOP). Thinking of the ice initiation from supercooled water clouds, not so many particles are detected as ice since the number of natural ice nuclei is generally scarce in the troposphere. So it is quite difficult to detect the signal of few ice crystals from the DOP frequency distribution. Even in the water clouds, there is certain amount of ranges of DOP, seeing from the Figs. 6a and 9a (I think that Fig. 4a must indicate the signals of aerosols, not water droplets. Please see the specific comment below.).

First, in the revised manuscript, we will add the following explanation on the factory calibration

process:

The rough-surface particles of 30–40 μm diameter are the spores of the *Lycopodium clavatum* Linnaeus provided by the Association of Powder Process Industry and Engineering (APPIE), Japan. Other rough-surface particles may also work; the key point is that we use certain particles so that we can calibrate the two detectors after the instrument is fully assembled. The sensitivity of the two detectors are differently adjusted so that the calibration particles give zero DOP on average (using 251 particle data). Typically, detector #2 is about three times more sensitive than detector #1; this is consistent with the fact that the polarization plate used has 34–35 % transmittance.

Second, in Figure R3-1, we show the DOP distributions obtained from the standard spherical particle experiments described in Appendix A. The results for the 5–30 μm particles are quite similar to the flight results for water clouds shown in Figures 4a, 6a, and 9a, namely, being distributed mostly at 0.3–1. For the smallest, 2 μm particles, the distribution is longer tailed to smaller (and negative) DOP values. For the 60 and 100 μm particles, whose I_{55} value was often saturated (as described in Appendix A), the distribution still resembles those for the 5–30 μm particles although it is somewhat longer tailed to smaller (but positive) DOP values. Figure R3-1 and corresponding discussion will be placed at the end of Appendix A of the revised manuscript.

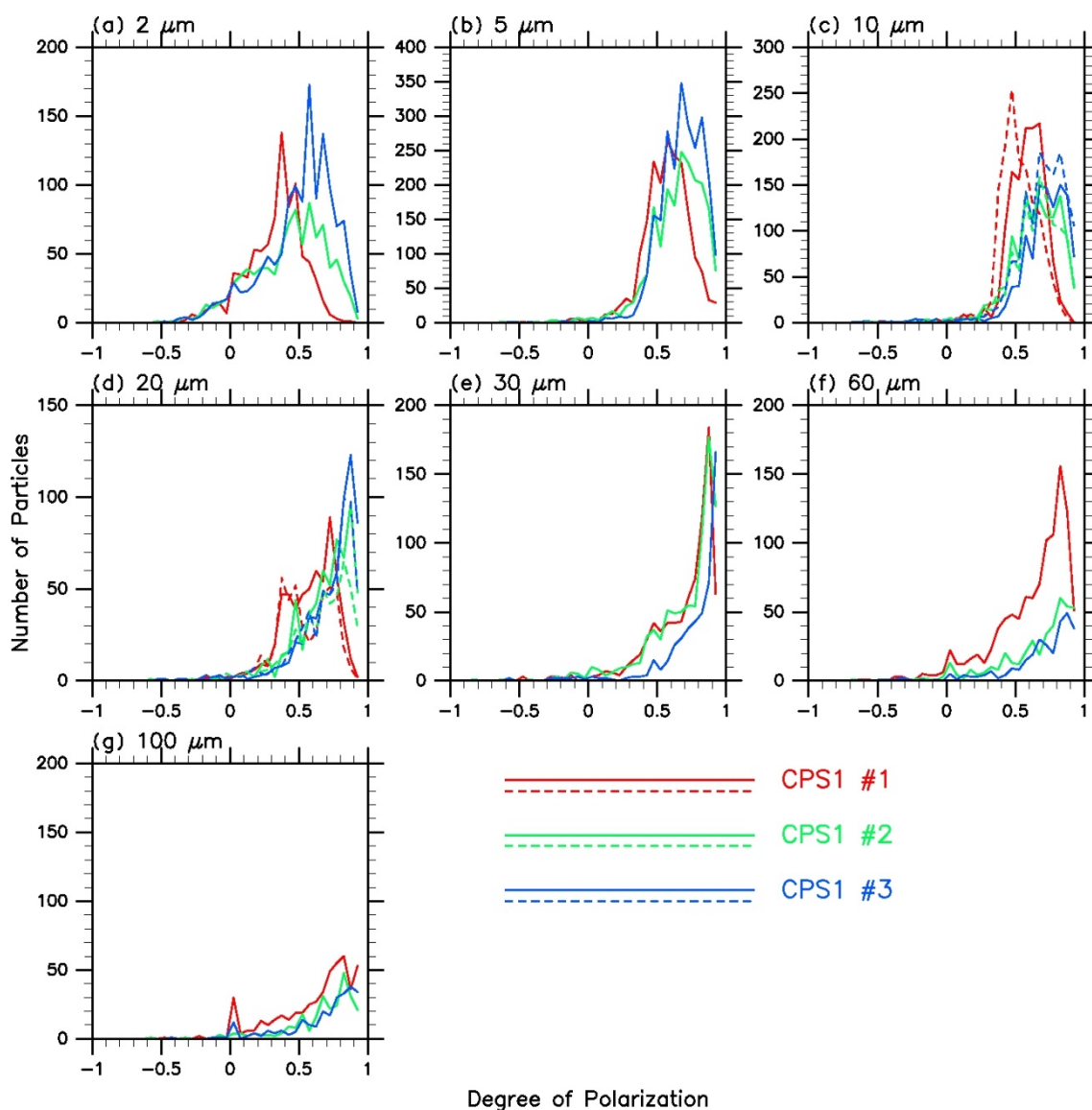


Figure R3-1. Frequency distributions of the degree of polarization (DOP) in 0.05 bins from the laboratory experiments using the standard spherical particles of (a) 2 μm , (b) 5 μm , (c) 10 μm , (d) 20 μm , (e) 30 μm , (f) 60 μm , and (g) 100 μm diameters. Red, green, and blue curves are for the CPS1 #1, #2, and #3 instruments, respectively. For the 10 μm and 20 μm particles (c and d), two sets of experiments on different days are expressed with solid and dotted curves.

Third, in the revised manuscript, we will discuss the relationship between the DOP value and the phase of cloud particle more carefully (by referring to the above Figure R3-1 as well) as follows:

When the DOP value is negative, the particle is ice. When the DOP value is positive but less than ~ 0.3 , the particle is most likely ice. When the DOP value is more than ~ 0.3 , the particle is water in many cases, but there is a chance that it is ice (because DOP can take values between -1 and $+1$ for ice particles; as shown in the flight results in the paper); for the final judgement, the DOP statistics of the

cloud layer to which the particle is belong and the simultaneous temperature value should also be taken into account (as done in the paper).

Finally, as pointed out by the Referee, there was a local dust event for the case shown in Figures 3 and 4. Please see below at your specific comment on this.

Or if the CPS has an advantage of counting of particles, the number concentrations in clouds, the sampling volume and counting efficiency are more thoroughly evaluated. To evaluate the sampling volume and its uncertainty during the ascent flight is essential to estimate the number concentration of particles. In the paper, only the rough estimate of detection area, $\sim 0.5 \text{ cm}^3$, is written in the text. Only the fixed typical ascent rate, $\sim 5 \text{ m/s}$, is used, although it will be variable from the surface to upper levels even in the same case.

As described in the manuscript, there is an upper limit in the number concentration directly measured by the CPS, though we have proposed a partial correction algorithm. Figure R3-2 shows the details of the detection area. As in the figure, the cross section of the detection area that the detectors effectively see is estimated as $\sim 1 \text{ cm} \times 1 \text{ cm}$, while its vertical extent is $\sim 0.5 \text{ cm}$.

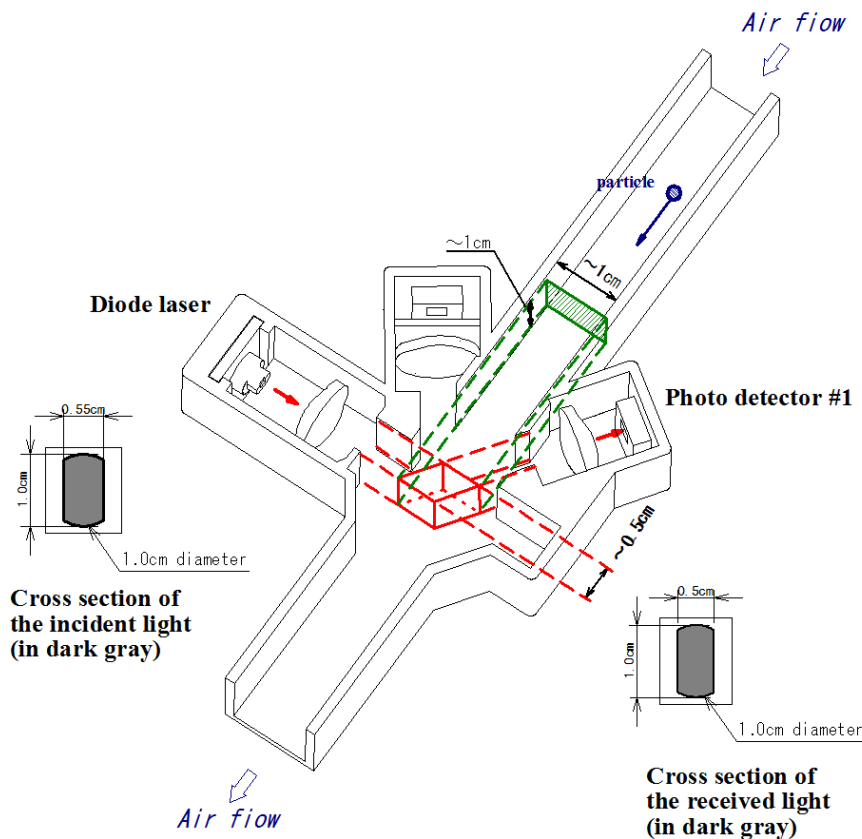


Figure R3-2. Schematic diagram of the CPS, showing the detection area in solid and dotted red lines.

Instead of using different flow speed values at different data points in a profile, we assume a constant flow speed of 5 m s^{-1} in this paper, and in the revised manuscript we will have a new appendix, Appendix C where we discuss the impact of different flow speeds on the number density conversion and the count number correction (see the next paragraph and Figure R3-3). In this way, the uncertainty in the number concentration values from the CPS is better understood, and the future CPS users can use this information to process and evaluate their data.

Planned Appendix C:

Both the conversion from number of particles $N [\text{s}^{-1}]$ to number concentration $C [\text{cm}^{-3}]$ and the correction factor for N depend on the flow speed within the detection area $v [\text{m s}^{-1}]$. As the cross section of the detection area is $\sim 1 \text{ cm}^2$, C is given by $N/(100v)$. As the vertical extent of the detection area is $\sim 0.5 \text{ cm}$, the correction factor for N (see discussion in Sect. 2.3) is $4 \times (psw/(5/v))^3$ if psw is greater than $5/v$, where psw is particle signal width in ms; if psw is smaller than $5/v$, the correction factor is unity. Figure C1 shows the relationships between N and C and between psw and the correction factor for $v = 3, 5,$ and 7 m s^{-1} . This indicates the contribution of the uncertainty in v (see also Appendix B) to the uncertainty in (corrected) N .

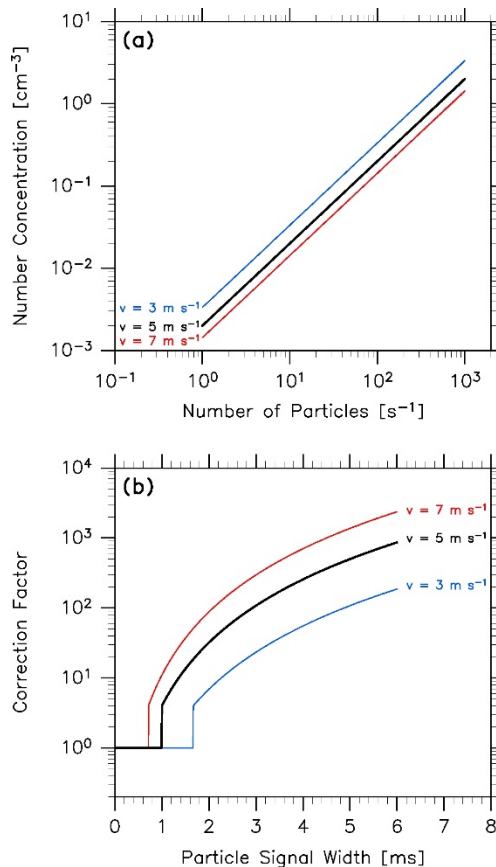


Figure R3-3. (Planned Figure C1.) Dependence on the flow speed within the detection area (v in m s^{-1}) for (a) the conversion from number of particles in s^{-1} to number concentration in cm^{-3} and (b) the correction factor for the number of particles (N in s^{-1}) with respect to the particle signal width values in ms. Shown are for 5 m s^{-1} (black), 3 m s^{-1} (blue), and 7 m s^{-1} (red).

Is the real counting efficiency considered to be uniform inside the cross section of detection area (1 cm x 1 cm)? Even if the intensity profile of a laser device and the air flow inside the area are assumed to be uniform, in fact, the efficiency and uncertainty of counting particle might not be distributed with uniformity between in the center and near the edge of the detection area. Does the intensity and peak wavelength of the laser change during the ascent or under different ambient conditions? If so, does it influence the measurement accuracy at what amount of uncertainties?

The counting efficiency may be roughly estimated by the cross section of the detection area (1 cm^2) divided by the cross section of the inlet duct (1.2 cm^2), being 83 %. Furthermore, the non-uniformity in the laser device may result in smaller efficiencies for smaller particles (particularly in the range $<30 \text{ }\mu\text{m}$). The temperature dependence of the laser light intensity was evaluated in a laboratory chamber using a CPS and changing the temperature from $+25^\circ\text{C}$ to -30°C . Note that during the actual flights (e.g. going through the cold tropical tropopause down to -90°C), the laser device is kept relatively warm thanks to the Styrofoam flight box and heat from the CPS circuit board; for example, during a flight the temperature in the flight box was -25°C when the air temperature was -70°C . The chamber result was that the detector output changed less than 2 % in this temperature range. We have not evaluated the temperature dependence of the laser peak wavelength. In Appendix A, we have taken the possible range (i.e. 775–810 nm) into account. The information in this paragraph will be included in the revised manuscript.

Moreover, how are the capabilities of measuring coarse aerosols (for instance, dust or sea-salt particles) in real atmosphere? In other words, does the CPS have the capability to distinguish among water droplets, ice crystals, and various types of coarse aerosols over the micron-sized range?

Any particles greater than $2 \text{ }\mu\text{m}$ are detected by the CPS. Please see below for the case in Figures 3 and 4.

Specific comments:

The following comments do not cover all general points above, but explain specifically as well as some minor points.

Page 3, Lines 19-20: Why the two photo detectors are placed at angles of 55 and 125 degrees? Do these set of angles have the best performance to distinguish between water droplets and ice crystals?

As written in the manuscript, we started the CPS development from the PS2 pollen sensor (with the detectors placed at 60 and -60 degrees). As we found that the lower detector for the PS2 type tends to be subject to wet contamination, we decided to move it to a higher place. There were two major considerations to determine the final two angles: (1) the laser device and the two detectors can be placed without difficulty in terms of assembling and production; and (2) the DOP distributions for spherical and non-spherical particles are well (similarly) separated as in the PS2 sensor.

Page 3, Lines 29-31: As for the calibration or ground test before the launch, in what ways is the sensitivity of both channels confirmed to be equal in terms of size measurements? In what ways is the calibration of polarization signal done quantitatively using the rough-surface particles? And the information on the rough-surface particles is required in the text (commercially available? mean size and its standard deviation? refractive index?).

As described above, the rough-surface particles used in the factory calibration process are the spores of the *Lycopodium clavatum* Linnaeus provided by the Association of Powder Process Industry and Engineering (APPIE), Japan. The sensitivity of the two detectors are differently adjusted so that the calibration particles give zero DOP on average (using 251 particle data). Typically, detector #2 is about three times more sensitive than detector #1; this is consistent with the fact that the polarization plate used has 34–35 % transmittance. The particles are commercially available, and of “30–40 μm ” diameter stated by the APPIE. Unfortunately, there is no information on the standard deviation of the size and the refractive index.

Page 4, Lines 1-11: The paper describes the laboratory data focused on the relationship between I55 and the particle diameter. The performance of I125 is also needed to be examined to show the accuracy and uncertainty.

Thank you very much for your suggestion. As written above, in the revised manuscript we will show the DOP distributions obtained from the laboratory experiments (see Figure R3-1).

Page 6, Line 5: Using the hot-wire anemometer sensor data, the flow speed in the duct is compared

with the balloon ascent rate. Thinking of the outlet area (3cm x 3cm) is wider than the inlet area (2cm x 2cm), what is the mechanism of significantly higher speed in the duct in some cases?

The uncertainty of the hot-wire anemometers used here is $\pm 1 \text{ m s}^{-1}$ ($k=2$). Furthermore, there may be additional flow of up to $\pm 2 \text{ m s}^{-1}$ due to the payload pendulum motions (depending on the length of the main string, payload configuration, and altitude).

Page 6, Lines 11-18: The actual maximum number counted per second is thought to be much smaller than the estimated maximum number (~1000) from limitation of the interface board. What was the maximum number per second measured from the test flight data (in water clouds)? The upper limit of number concentrations in the CPS measurements can be much smaller than $\sim 2 \text{ cm}^{-3}$? The typical number concentration of cloud droplets in natural clouds covers from tens to thousands of particles per cubic centimeter, so basically is it difficult to reliably measure the number concentrations of water clouds even with development of any correction algorithms?

In water cloud, $\sim 200 \text{ s}^{-1}$ for midlatitude precipitating clouds (Figure 5) and $\sim 300 \text{ s}^{-1}$ for tropical low level cloud layer (Figure 8) were obtained. They are uncorrected values.

Page 8, Lines 22-23: The manuscript states that there is a cloud layer from the surface to $\sim 2 \text{ km}$. However it is considered more reasonable that the signal should indicate the layer of coarse aerosols (possibly in swollen state) since the RH is subsaturated with respect to water and it is inconceivable to have very low concentrations for cloud water droplets in the subsaturated layer. That is why I think it is quite difficult to determine the cloud phase only from the DOP frequency distribution.

As described in Page 9, lines 5–8, there was a local dust event on the day of flight (18 March 2013) due to strong surface wind in association with a low pressure system. This is supported by surface observations of enhanced suspended particulate matter (SPM; particles equal to or smaller than $10 \mu\text{m}$) at five sites located 3–14 km from the launch site (data obtained from the environmental database of the National Institute for Environmental Studies (NIES)). Sugimoto et al. (2016) also discussed this local dust event based on depolarization-lidar and surface particle ($\text{PM}_{2.5}$ and PM_{10}) measurements at Tsukuba (at NIES; 36.05°N , 140.12°E), which is located $\sim 16 \text{ km}$ from the launch site. These dust particles are mineral dust blown up by the strong wind from unplanted fields in this area. On the other hand, surface precipitation data are available every 10 minutes at Tsukuba (also called as Tateno) site of the Japan Meteorological Agency (36.06°N , 140.13°E ; also $\sim 16 \text{ km}$ from the launch site). The data record indicates that there was no precipitation at the surface up to 19:50 LT, and after 20:00 LT there was precipitation of less than 0.5 mm. Figure R3-4 shows the results from the depolarization lidar

measurements at Tsukuba (NIES) between 06:00 LT and 24:00 LT on 18 March 2013 (Sugimoto et al., 2008, 2016; <http://www-lidar.nies.go.jp/AD-Net/>, accessed 15 August 2016). This lidar system uses 532 nm and 1064 nm laser light, with the depolarization measurement capability at 532 nm. It takes 15 minutes for one cycle of the measurement, including 5-min laser-light emission and 10-min temporary pause. The vertical resolution of the data is 30 m. Figure R3-4 shows that the local dust event, confined up to ~0.5 km, started around 09:00 LT and ended around 19:00–20:00 LT. The dust particles have depolarization ratios of ~15–30 %. On the other hand, at 18:00 LT, low-level clouds appeared whose base was estimated to be located at 0.72 km, and the cloud base descended gradually afterwards. These clouds are characterized by large backscatter coefficients (greater than $1 \times 10^{-5} \text{ m}^{-1} \text{ sr}^{-1}$) and small depolarization ratios (less than 10%). The two CPSs were launched at Moriya (35.94°N, 140.00°E) at 18:07:44 LT. Therefore, these CPSs should have encountered mineral dust particles (which might have been somewhat wet) up to ~0.5 km and water cloud particles above ~0.7 km.

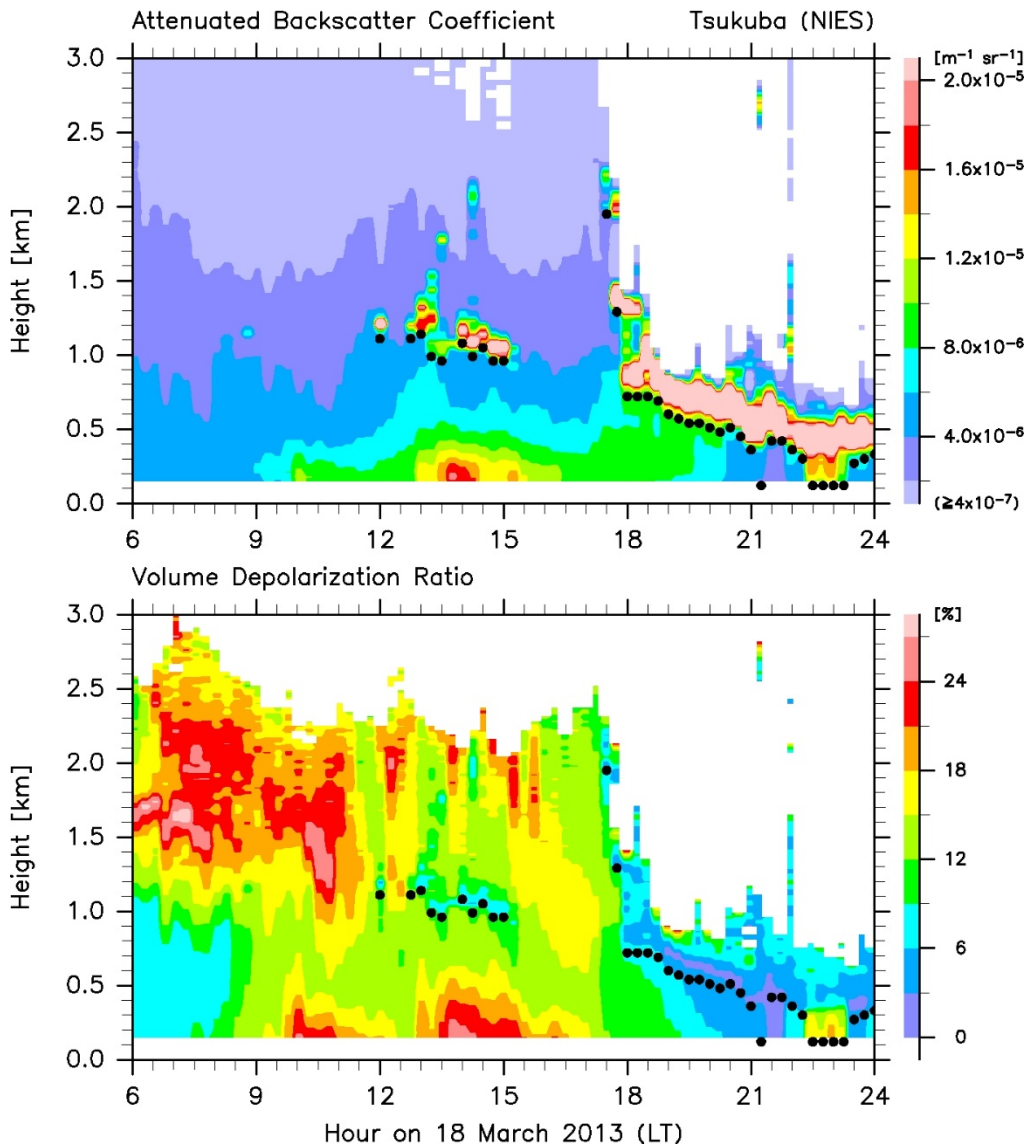


Figure R3-4. Time-height distributions of attenuated backscatter coefficient at 532 nm (top) and volume depolarization ratio at 532 nm (bottom) measured with the lidar system at Tsukuba (36.05°N , 140.12°E) between 06:00 LT and 24:00 LT on 18 March 2013. Temporal resolution is 15 minutes, and vertical resolution is 30 m, with the lowest 120 m portion of the data not shown because of large uncertainty. For the depolarization ratio plot, data points whose 532 nm backscatter coefficient is $<1.0 \times 10^{-6} \text{ m}^{-1} \text{ sr}^{-1}$ are not shown. Also shown with dots in both panels are the cloud base location estimated from the 1064 nm lidar measurements (i.e. the lowest level where vertical gradient of 1064 nm attenuated backscatter coefficient exceeds $1.2 \times 10^{-6} \text{ m}^{-1} \text{ sr}^{-1}$ per 60 m; and the maximum attenuated backscatter coefficient in the cloud layer must exceed $2.0 \times 10^{-5} \text{ m}^{-1} \text{ sr}^{-1}$, with apparent cloud top where attenuated backscatter coefficient value becomes equal to that at the cloud base.).

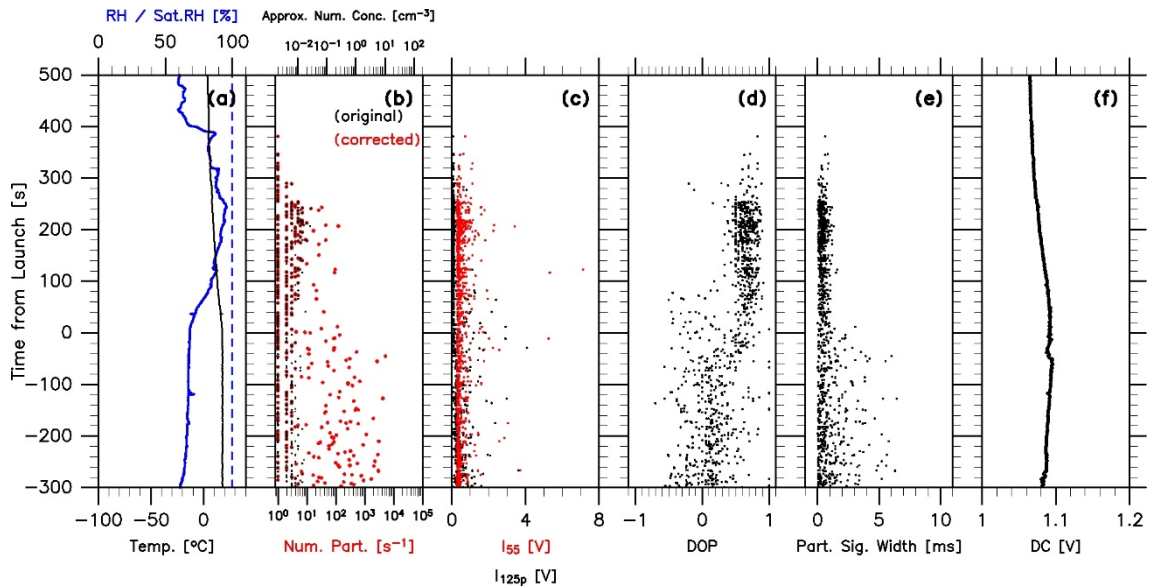


Figure R3-5. As for Figure 3 in the originally submitted manuscript, but with time in vertical axis, between -300 s before the launch and +500 s after the launch (time 0 corresponds to the launch time). Results from one of the two CPSs (the CPS1 type) at Moriya, Japan, launched at 18:07:44 LT on 18 March 2013. Time series are shown of (a) temperature (black), RH (blue solid), and ice saturation RH (dashed blue) from the RS-06G radiosondes, (b) number of particles counted per second (and number concentration assuming 5 m s^{-1} flow speed), original in black and corrected in red, (c) particle output voltages I_{55} (red) and I_{125p} (black), (d) the degree of polarization (DOP), (e) particle signal width in ms, and (f) the DC component from the detector #1 output.

Figure R3-5 shows the results from one of the two CPSs (the CPS1 type) during the period between 300 s before the launch and 500 s after the launch (around 2.5 km). The CPS was placed outside at the surface from ~ 300 s before the launch. The results show that before the launch (i.e. at the surface), the CPS detected particles whose DOP is distributed widely between -1 and $+1$ and that after the launch, the DOP became much more confined to ~ 0.5 – 0.9 . The former group of particles are considered to be the mineral dust particles, and the latter group of particles are mostly spherical particles, i.e. mostly water cloud particles.

In the revised manuscript, we will add the above descriptions and discussions including Figure R3-4. It is true that the CPS would not be able to distinguish between spherical non-water particles (e.g. the standard spherical particles used in the laboratory experiments) and water particles only from the DOP information. Other information such as radiosonde temperature and RH measurements and independent particle measurements is sometimes necessary for this distinction. It should be noted that the uncertainty of the RS-06G and RS-11G RH measurements is $\pm 7\%$ RH (this information will also be added in the revised manuscript). Also, water cloud particles can exist temporarily in subsaturated layers when, e.g. they are falling from the above. Finally, we will revise Figure 4 of the originally

submitted manuscript by changing the height region for water clouds from 0.5–1.5 km to 0.8–1.5 km (see Figure R3-6). Essentially, the results do not differ between the original Figure 4(a) and Figure R3-6(a).

Reference:

Sugimoto, N., Shimizu, A., Matsui, I. and Nishikawa, M.: A method for estimating the fraction of mineral dust in particulate matter using $PM_{2.5}$ -to- PM_{10} ratios, *Particuology*, 28, 114–120, doi:10.1016/j.partic.2015.09.005, 2016.

Sugimoto, N., Matsui, I., Shimizu, A., Nishizawa, T., Hara, Y., Xie, C., Uno, I., Yumimoto, K., Wang, Z., Yoon, S.-C.: Lidar network observations of tropospheric aerosols, *Proc. SPIE 7153, Lidar Remote Sensing for Environmental Monitoring IX*, 71530A (December 09, 2008), doi:10.1117/12.806540, 2008.

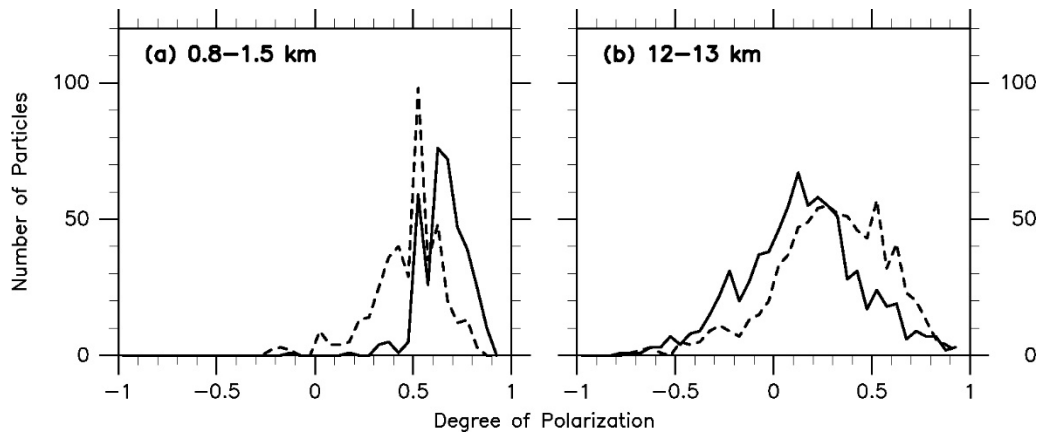


Figure R3-6. Revised Figure 4 of the originally submitted manuscript. The height range for (a) has been changed from 0.5–1.5 km to 0.8–1.5 km.

Page 11, Lines 21-29: Although it might be impossible to compare the figures related to depolarization between the CPS and the remote-sensing measurements, is there any way to evaluate the DOP uncertainty? The comparison with other airborne sensors in laboratory experiments is useful to show the CPS performance for depolarization.

The DOP uncertainty can be evaluated by the laboratory experiments using standard spherical particles. Please see above (and Figure R3-1). It is impossible to relate the CPS's DOP values to the lidar depolarization ratio values. We are happy to participate in future laboratory and field intercomparison projects.

Pages 13-14 (Appendix A): The laboratory experiments are described using the standard spherical particles with different types and sizes. The description on how to enter the particles into the detection area is also required in the text. Is the air vacuumed from the bottom of the particle inlet duct at 5 m/s? How do the particles dispense before entering the particle inlet? Are there any calibration data to be described using non-spherical particles? That might be helpful to show the uncertainty of the CPS polarization measurement.

The air was not vacuumed. We used a special apparatus to introduce the particles separately with a fan that pushes air downward into the CPS. Non-spherical particles were not used in the laboratory experiments, but as described above, the rough-surface particles are used during the factory calibration process.

Thank you very much again for your comments and suggestions. Please also see the discussion with the other two referees.